Desalination and Water Treatment
www.deswater.com
doi: 10.5004/dwt.2023.29693

299 (2023) 269–276
July

Monitoring of interannual variabilities of glacial lakes at the end of A'nyemaqen glacier utilizing Pol SAR images

Rui Guo*, Qiming Zeng

Institute of Remote Sensing and Geographic Information System, School of Earth and Space Sciences, Peking University, Beijing 100871, China, emails: grace20230525@163.com (R. Guo), qmzeng@pku.edu.cn (Q. Zeng)

Received 10 November 2022; Accepted 21 May 2023

ABSTRACT

Due to climate change in recent years, the degradation of most glaciers on the Qinghai–Tibet Plateau has accelerated the expansion of glacial lakes. Based on the polarization entropy difference between water and non-water signals, this paper studies the classification method of glacial lake in snowmelt period by using the dual-polarization time series synthetic aperture radar (SAR) images as data sources, and proposes a method for extracting and dynamically monitoring glacial lake based on the normalized polarization entropy ratio of dual-polarization SAR images. In order to verify the feasibility of the method, the Sentinel-1 dual-polarization image sequence of ESA was selected to carry out the dynamic extraction of glacial lakes and the analysis of long-term temporal variations on a time span of 4a for the typical experimental area located in the glacier basin of A'nyemaqen. The spatial and temporal changes of the glacial lake at the end of the A'nyemaqen glacier during 2019–2022 were successfully obtained through experiments, and then it was found that the area of the glacial lake near 4a was decreasing.

Keywords: Synthetic aperture radar (SAR); Glacial lake; A'nyemaqen glacier; Dual-polarization; Remote sensing classification

1. Introduction

Glacier lakes hold significant importance on a global and regional scale due to their vast water resources, as stated by Gao et al. [1]. Along with the formation of new glacier lakes comes the potential for various opportunities, such as geosystem services, but also the emergence of risks like floods [2]. Glacial mountain regions are among the most sensitive and vulnerable to climate change in the world [3]. Uncertainties persist regarding the harm potential of glacial lakes, especially with atmospheric warming and accelerated glacial retreat in alpine regions [4].

Because the glacial lakes are mostly distributed in high altitude remote mountainous areas, the field investigation is difficult and costly. The common technical approaches based on optical remote sensing image are supervised classification and unsupervised automatic classification based on various indices or image texture features [5]. Thematic analysis of glacial lakes through optical images is limited due to the constant cloudy, wet, and rainy climate, resulting in scarce available data and a data source bottleneck. However, the use of satellite synthetic aperture radar (SAR) sensors has gained significant attention in recent years due to its ability to operate in various weather conditions. SAR remote sensing has great potential for monitoring large-scale surface displacement deformation and land cover changes [6–10].

At present, the research of glacier movement and ablation monitoring based on SAR remote sensing has made great progress [11,12]. SAR data's application to glacial lakes development and outbursts remains in its infancy, with few scientific achievements. Intensity-based classification methods encounter problems of difficult threshold determination, low classification accuracy due to white

* Corresponding author.

Gaussian noise in flood and water monitoring [13]. To solve this problem, Zhang et al. [14] proposed a method of glacial lake extraction and dynamic monitoring based on normalized intensity ratio of time-series SAR images. The principle is based on the specular reflection and low backscattering when the water surface is calm.

However, glaciers and their lakes in cold high latitude regions freeze in winter. During snow coverage or melting, similar scattering characteristics result in greater image brightness due to volume scattering of snow. The normalized ratio method based on intensity is invalid. Unipolarized radar relies on echo scattering amplitude while polarized radar records scattering echo as a matrix, including scattering amplitude and phase information. Compared with single-polarized SAR, polarimetric SAR (polarimetric SAR) can reflect the polarization scattering characteristics of ground objects [15]. Identifying distinct scattering mechanisms can improve target recognition accuracy. There are precedents for water extraction and dynamic assessment based on Pol SAR polarization classification [13]. Polarimetric SAR sensors provide better glacier monitoring with their sensitivity to water content and surface roughness, compared to single-polarization sensors. However, acquiring full polarization data is limited, making systematic research difficult. Sentinel-1A's launch in 2014 improved this with free dual-polarization data, offering greater long-term data availability for glacier change monitoring.

Polarizing target decomposition (TD) technique is one of the most widely used methods in Pol SAR data analysis [16], which is the most effective way to analyze the scattering characteristics of a target. Target decomposition breaks down polarization scattering matrices, expressing them as basic scattering mechanisms to improve target image understanding. Therefore, this study introduces a method using polarization entropy normalized ratio to dynamically monitor glacial lakes, based on sequential polarization entropy images. Polarization entropy describes the complexity increase within the target during snow and ice melting periods, a crucial time for glacial lake water storage changes. The standardized ratio method based on target polarization entropy is applied for monitoring the typical range of glacial lakes in the A'nyemaqen glacier basin. The method's feasibility is verified by examining the glacial lakes in the southwest region of the A'nyemaqen basin using 98 Sentinel-1 dual-polarization images over 2019–2022.

2. Study area and materials

2.1. Study area

The A'nyemaqen Iceberg, located in the north of the Qinghai-Tibet Plateau, is the Yellow River's headwater and a section of the Eastern Kunlun Mountains. It spans 125 km^2 and has valley glaciers on the southern slope, susceptible to ice avalanche and debris flow. A'nyemaqen produces melting water from glaciers, providing water resources for Yellow River tributaries and replenishing the southwest slope's surface water system with ice and snow melt and precipitation. Our study focuses on a group of dozens to hundreds of individual glacial lakes on the southwest slope of the glacier, mainly moraine lakes and thermal melting ponds.

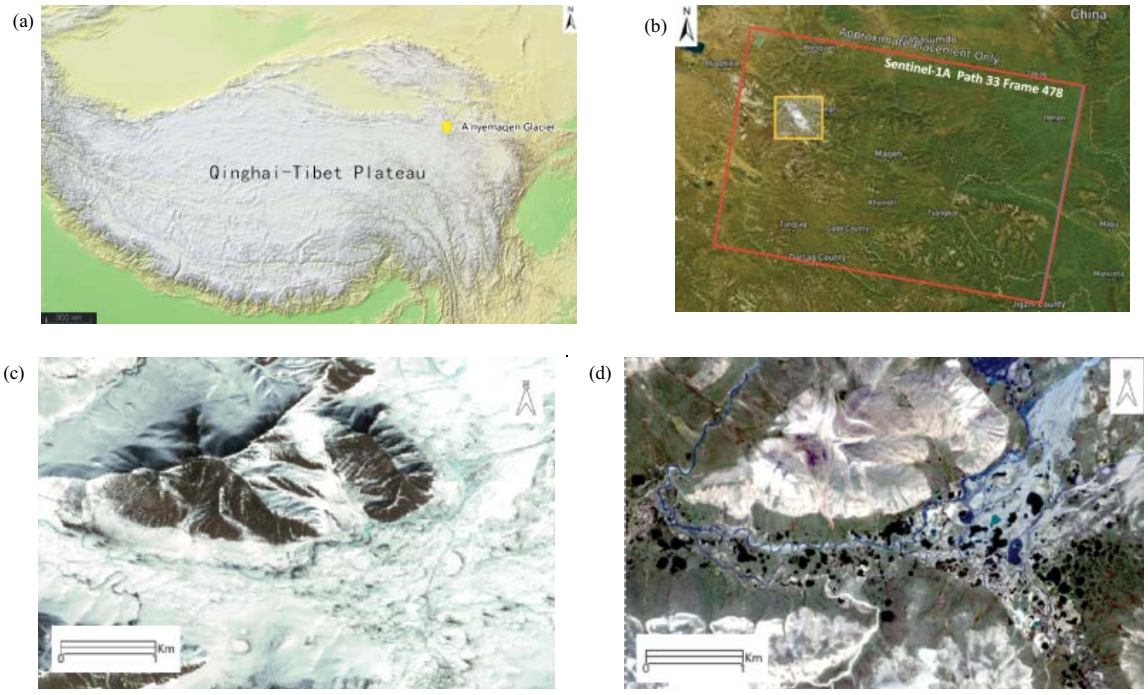

Fig. 1. Study area and data overview. (a) The location of the A'nyemaqen glacier on the Tibetan Plateau, (b) the yellow box is the scope of the study area, and the red box is the coverage of SAR image, (c) Gf-1 optical image of glacial lake at the end of A'nyemaqen glacier (imaging time: Feb 3, 2021) and (d) Gf-1 optical image of glacial lake at the end of A'nyemaqen glacier (imaging time: July 7, 2021).

Located in the hinterland of the Qinghai-Tibet Plateau, the A'nyemaqen Iceberg has a typical plateau continental climate [17]. Affected by the East Asian monsoon, Icebergs in A'nyemaqen have a large amount of rainfall (snow) and a large amount of evaporation. The precipitation mainly concentrates in summer, accounting for 56% to 62% of the annual precipitation [18]. A'nyemaqen Iceberg's steep terrain is vulnerable to north and northwest cold currents, with an annual average temperature of –10.2°C. The warm season between May and September has rain and heat, gathering precipitation and snow melt water quickly. The cold season between October and April is often covered by ice and snow, with temperatures reaching below –50°C in January.

2.2. Pol SAR data source

In order to obtain the continuous temporal sequence changes of the A'nyemaqen glacier in 2019–2022, considering the position and coverage of the study area on the image, the Sentinel-1's C-band IW mode dual-polarization orbit drop data was used, with a spatial resolution (single view) of 5 m × 20 m and a width of 250 km. A total of 98 images were obtained from January 2019 to December 2022, polarized by VV and VH.

3. Glacial Lake extraction

3.1. Data preprocessing

In order to avoid the accumulation of registration errors in the subsequent processing of single image pairs, all SAR data should be registered first. The image collected on January 8, 2021 was selected as the main image, and the whole data set was registered.

The effect of speckle noise can be mitigated by a common multi-look step at the expense of spatial resolution. In this study, the images of the same scene with long time series in different periods are available, so the De Grandi filter is used on the basis of multi-view to conduct multi-temporal filtering for the registered radar images, which can enhance the time and space changes in the case of a large number of time observation data [19]. The De Grandi filter can use local spatial statistics to balance the reflectance differences between images at different times. The filter is used in both time and space domains. Since wavelet-based estimators preserve structures in the image (such as edge and point targets), these structures and their variations are also preserved on average across the time domain.

3.2 Extraction of SAR dual-polarization temporal scattering characteristics based on H-α anisotropy decomposition

The sensitivity of polarimetric SAR sensors to water content and surface roughness enables them to provide more information for glacier monitoring than single polarimetric SAR sensors. Polarized radar simultaneously transmits and receives H and V polarized wave pulses, recording the backscatter information of each resolution unit on the ground. The polarization scattering matrix unifies energy, phase, and polarization characteristics to describe the electromagnetic scattering characteristics of a radar target, improving imaging radar's abilities to acquire information about the target. This allows polarization radar to extract various polarization information to identify and classify ground objects and extract surface parameters, such as dielectric constant and surface roughness, revealing the polarization response characteristics of ground objects [20–22].

For Sentinel-1 double polarization data, the Dual Polarimetric Entropy Alpha Anisotropy Decomposition method was used to decompose the coherence matrix of the polarized SLC dataset. The Polarization Scattering Matrix of SAR image is a matrix that describes scattering characteristics of SAR signal in different polarization states, also known as Polarimetric Scattering Matrix [20]. Based on the dual-polarization scattering matrix, the target covariance matrix was decomposed and the total backscattering coefficient was decomposed into cross scattering and other scattering parts. In order to analyze the disorder of ground object scattering process, Cloude et al. [20] introduced target scattering polarization entropy:

$$H = -\sum_{i=1}^{2} P_i \log_2 P_i \tag{1}$$

where $P_i = \frac{\lambda_i}{\lambda_1 + \lambda_2}$, λ_i represents the eigenvalue of the covariance matrix, and represents the intensity of a scattering mechanism. Target scattering polarization entropy is a measure of target disorder [23]. It is related to the randomness of the scattering process, and its value ranges from 0 to 1. H = 1 for random targets and 0 for simple (single) targets. Specifically, when the polarization entropy is low, it can be considered that there is only one dominant scattering mechanism. When the polarization entropy is equal to 0, it can be considered that the scattered wave is completely polarized, and the ground object can be considered as a simple target, a single target or a deterministic target. When the polarization entropy is high, the scattering mechanism tends to be random. When the polarization entropy is equal to 1, the scattered wave is completely depolarized and it can be considered as a completely random target.

Various factors can influence the differences in radar backscattering observed in multi-period and multi-polarization SAR data, such as changes in land cover, variations in the observation geometry, differences in surface topography, the polarization configuration used, and variations in

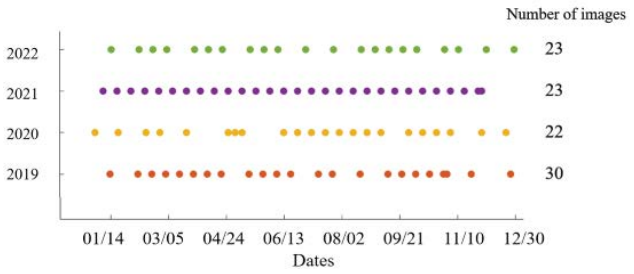

Fig. 2. Temporal distribution and number of Sentinel-1 images in the study zone.

meteorological conditions [24]. Some parameters, such as the content of liquid water in the covered snow, snow particle size and surface roughness, will change when the snow on the surface of the glacial lake is melted or the lake is stored. In each pixel, due to the heterogeneity of geometric features and dielectric properties such as ground slope, roughness and dielectric constant, as well as the influence of surface vegetation, the pixel can also be regarded as a collection of several single small scatters, and the backscattering of the pixel is the statistical average of these small scatters [25].

3.3. Glacial lake extraction from time series dual-polarization SAR images

When the snow covering the glacier ice starts to melt, the scattering mechanism inside the target increases in complexity, and the polarization entropy can well describe this phenomenon, and the snow and ice melting period is an important period for the change of the glacial lake water storage. Therefore, this paper supplemented the above intensity normalized ratio method through the polarization entropy extracted by the bipolarization decomposition, and carried out the action in the typical glacial lake range in the A'nyemaqen glacier basin state monitoring. The proposed method is called standardized ratio method based on target polarization entropy. Typical glacial lakes in the southwest of the A'nyemaqen glacier basin were selected and the data in 2021 were taken as an example for experiments to verify its effectiveness. The technical process is as follows as Fig. 3.

Creating a standard polarization entropy image S_i by averaging polarization entropy images from the cold season of glacial lakes and the surrounding, snow-covered surface.

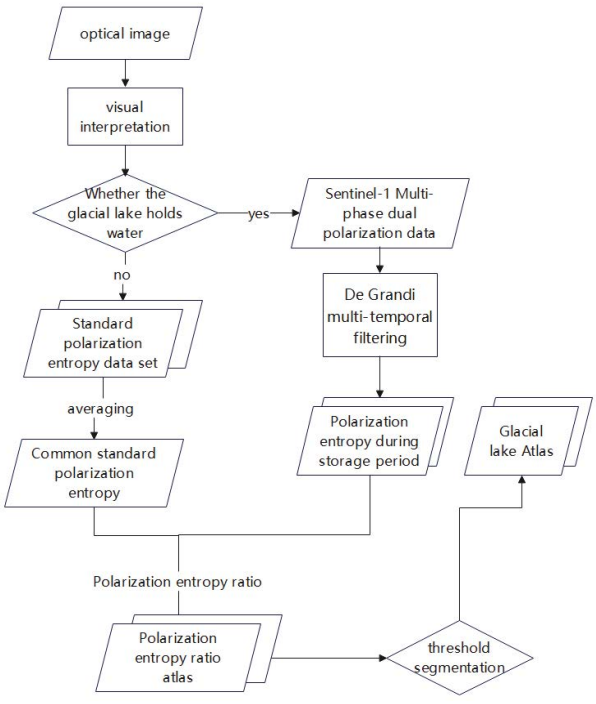

Fig. 3. Flowchart for dynamic extraction of glacial lakes using entropy standardization ratio of sequential SAR images.

And H_i means the polarization entropy of radar image at different times. As shown in the formula, the standardized polarization entropy ratio R_i is obtained, and then the time sequence change of polarization entropy is detected.

$$R_i = \frac{H_i}{S_i} \tag{2}$$

3.4. Temporal classification and extraction of glacial lake water

Firstly, the long-term Pol SAR image registration, tailoring, filtering, polarization target decomposition and geocoding are carried out to obtain the long-term Pol SAR polarization entropy data set. Through visual interpretation of optical images in the study area, it is confirmed that the subsets of polarization entropy data in November and December in winter are common standard images. Taking Sentinel-1A images acquired in 2021 as an example, the ratio of temporal SAR image polarization entropy to common standard image polarization entropy and the ratio of temporal SAR image intensity to common standard image intensity were calculated, as shown in Fig. 4.

After impoundment of the glacial lake at the end of the A'nyemaqen glacier, the contrast between the water body and the non-water body is obvious. Due to the sensitivity of polarization entropy to glacial lakes during snowmelt period, the ratio of glacial lakes in the left figure changed significantly from March to June, while the scope of glacial lakes was not detected in the right figure during this period. At different imaging moments, the ratio of the non-water area fluctuated in the interval (0,2), because the scattering characteristics of the moraine in the non-water area were relatively stable. As for the water body area, although the presence of lake water caused the difference in the scattered signals in the lake area, the distribution range of water body was relatively consistent in the ratio image of each period.

It can be seen from the figure that the polarization entropy ratio of the glacial lake at the end of the glacier in the A'nyemaqen glacier basin changes significantly after water storage. In September and October, the intensity standard ratio method extracted a small range of glacial lakes, while the polarization entropy ratio method was fuzzy in the image. However, the polarization entropy ratio method extracted the obvious glacial lake range in March, April and May, while the intensity standard ratio method extracted the glacial lake range in this time range is fuzzy, even did not identify the glacial lake. This is because in this time range, the temperature gradually rises, but the snow cover on the surface of the glacial lake is not completely melted. According to the visual interpretation, the range of the glacial lake is effectively extracted by the polarization entropy ratio method from March to August, which makes up for the omission of the intensity standard ratio method from the glacial lake extraction during the ice and snow melting period. According to the maximum polarization entropy standard ratio and intensity standard ratio of the glacial lake and the edge of the glacial lake, 2 and 1.8 were selected as the best thresholds after several experiments, and the results obtained by the two methods were segmented to extract the temporal variation of the glacial lake area.

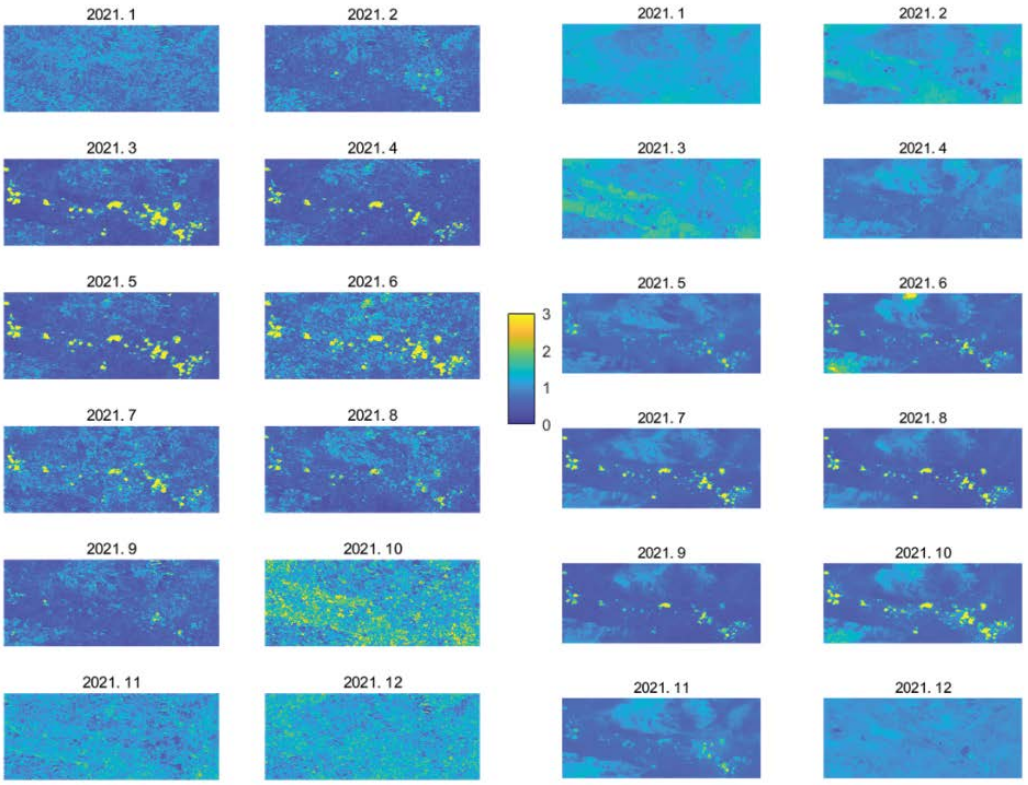

Fig. 4. Two columns on the left are the ratio of polarization entropy of time-series SAR images to common standard image polarization entropy, and the two columns on the right are the intensity standardized ratio of single-polarization time-series SAR images [14].

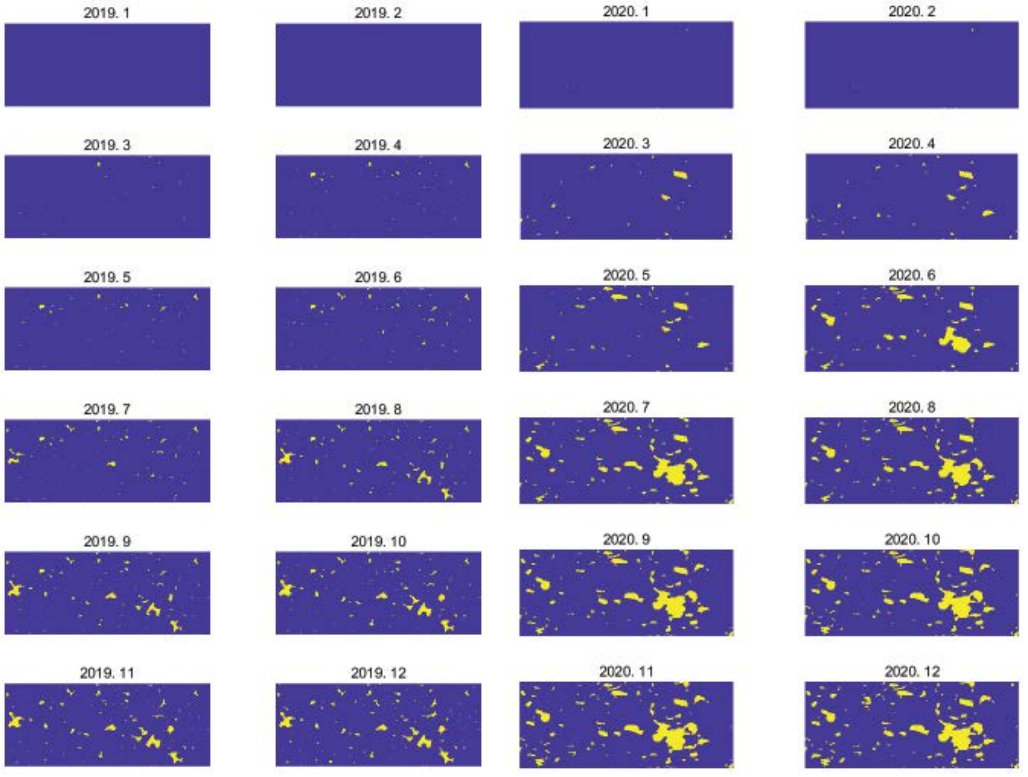

Fig. 5 (Continued)

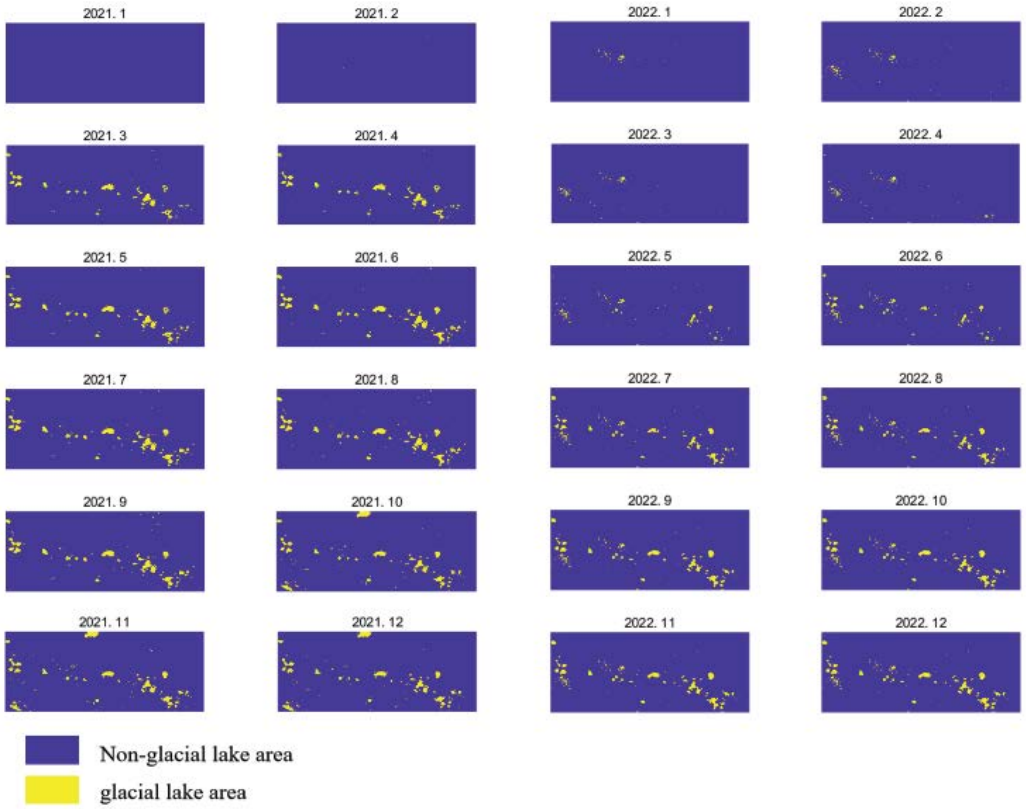

Fig. 5. A time-series classification map of glacial lakes represented in the A'nyemaqen glacier basin in 2019–2022.

4. Results

4.1. Temporal and spatial variations of glacial lakes at the end of A'nyemaqen glacier

Fig. 5 displays the classification outcomes for water and non-water areas of glacial lakes in the study region. The yellow area is the temporal distribution range of glacial lake.

From 2019 to 2022, the area of the glacial lake group is similar in general, gradually increasing from March to June each year, and then basically staying the same. The glacial lake area after threshold segmentation is multiplied by the ground size represented by each pixel to convert the binary image into the glacial lake area. In 2019, the total area was the smallest, 8.52 km^2. In 2020, the total area nearly doubled, reaching the maximum of 17 km^2 in the past 4 y. The glacial lake area increased, and many scattered small lakes became one in this year. In the following 2 y, the total area decreased year by year, reaching 14.29 and 9.59 km^2. The change rates of the total area were 99.59%, –16.00%, –32.86%, and the change rates of the largest area were 0.29%, –0.36%, –0.19%, respectively (as shown in Table 1).

4.2. Relationship of glacial lake at the end of A'nyemaqen glacier to temperature and rainfall

According to the threshold segmentation results of standardized polarization entropy ratio, the dynamic distribution of glacial lake was obtained, and the relationship between glacial lake area change and temperature and precipitation was analyzed, and the time series curve was drawn, as shown in Fig. 4. The variation pattern of glacial lake area is similar to that of temperature and precipitation, both of which increase in summer every year. However, the changes of glacial lake area and temperature and precipitation are not completely synchronized. On the whole, the increase time of glacial lake area is later than that of temperature and precipitation. This may be due to precipitation and melting of ice and snow replenishing the glacial lake, a process that accumulates over time.

From December to March of the following year, the temperature of the A'nyemaqen glacier is below zero, and the glacier hardly melts, and the rainfall distribution is less, and the water level of the glacial lake gradually decreases, until the lake disappears completely in February. In April, the rainfall began to increase, the temperature warmed to above zero, and the snow and ice began to melt. In May, the melting water of the A'nyemaqen glacier gathered, and in June, the snow in the high mountain belt melted, and the runoff appeared in spring flood, accelerating the storage of the glacial lake.

According to the curve distribution of lake area, temperature and rainfall, the water storage and outburst of the glacial lake are highly correlated with the change of temperature and rainfall, so it can be inferred that the melting period of the A'nyemaqen glacier is from April to October, which is two months longer than the melting period of the Tibetan Plateau glacier (from May to September).

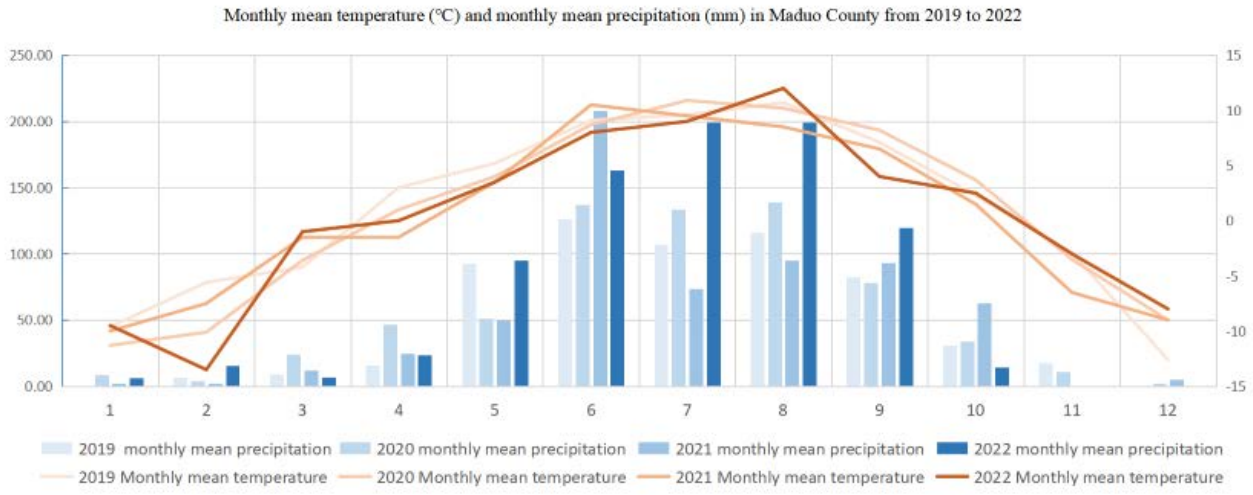

Fig. 6. Monthly mean temperature (°C) and monthly mean precipitation (mm) in Maduo County from 2019 to 2022.

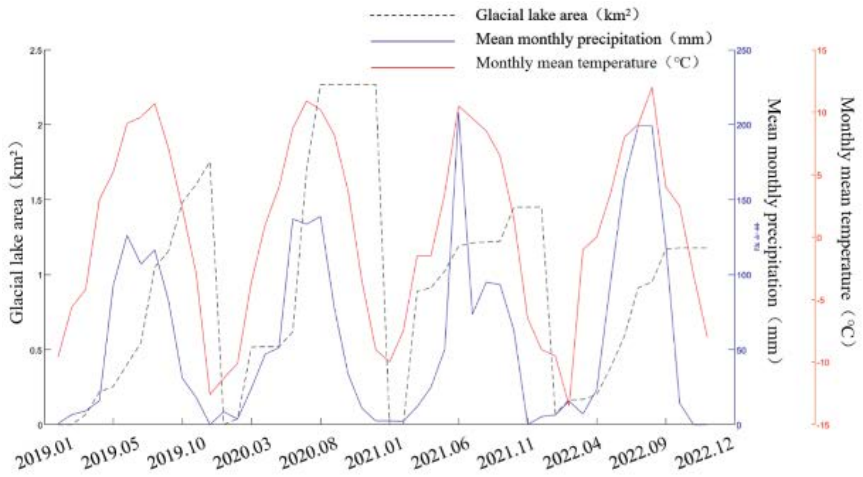

Fig. 7. Time sequence curve of glacial lake area change.

Table 1
Glacial lake area change

	2019	2020	2021	2022
Maximum glacial lake area (km²)	1.75	2.27	1.45	1.18
Glacial lake area (km²)	8.52	17.00	14.29	9.59

5. Conclusion

In this paper, we proposed a technique for extracting and monitoring glacial lakes using time-series SAR images, which relies on the polarization entropy standardized ratio. Moreover, the glacial lake group located in the southwest of the A'nyemaqen glacier was selected as the experimental object, and 98 scenes were successively acquired by the sentine-1a of the European space agency The spatial and temporal distribution of the two large glacial lakes at the end of the A'nyemaqen glacier during 2019–2022 were extracted with SAR images, and the change process and trend of the experimental subjects in recent years were summarized and analyzed.

First of all, the experimental study on the A'nyemaqen glacier in this paper highlights the prominent advantages of SAR satellite not restricted by the bad weather conditions of clouds and mists, and the high repetition period provides stable and reliable high-potential data support for the dynamic monitoring of glacial lake outburst and related remote sensing applications of plateau mountains. The potential of polarization information in ice and snow remote sensing is fully exploited by the method of polarization target decomposition. Secondly, through analysis of the time-series polarization entropy, it was discovered that the polarization entropy can sensitively detect glacial lakes during the melting season, which led to proposing a method for extracting the glacial lake area change by using a ratio of polarization entropy and standard polarization entropy derived from time-series SAR images in addition to the intensity standardization ratio method for extracting the periodic water storage area of glacial lakes. This approach

effectively eliminates the influence of thermal noise and counteracts the interference from complex terrain, while also magnifying the differences between glacial lake and non-aqueous signals during the melting season, preventing confusion between ice and water in winter and providing supplementary reference for water body segmentation methods based on intensity, ultimately ensuring the accuracy of water body segmentation.

The experimental results show that the storage area of the glacial lake at the end of the A'nyemaqen glacier has increased from 8,520 to 17,000 m^2 in the past 4 y, and then dropped to 95,900 m^2 in 2022. It is found that the glacial lake at the end of the A'nyemaqen glacier has a relatively stable life cycle through the analysis of the long interannual changes. Although glacial lakes are influenced to some extent by temperature changes and fluctuations in rainfall within glacial regions, they typically begin to increase around March to April, reach their maximum size around October, and eventually dry up in January to February of the following year. The above conclusions can be used as reference for the research of polarimetric SAR in glacial lake field and also provide basic data for the research of related secondary geological disasters in this region.

References

[1] Y.P. Gao, S.Y. Liu, M.M. Qi, F.M. Xie, K.P. Wu, Y. Zhu, Glacier-related hazards along the International Karakoram highway: status and future perspectives, Front. Earth Sci., 9 (2021) 611501, doi: 10.3389/feart.2021.611501.

[2] C. Viani, N. Colombo, I.M. Bollati, G. Mortara, L. Perotti, M. Giardino, Socio-environmental value of glacier lakes: assessment in the Aosta Valley (Western Italian Alps), Reg. Environ. Change, 22 (2022) 7, doi: 10.1007/s10113-021-01860-5.

[3] A. Juřicová, S. Fratianni, Climate change and its relation to the fluctuation in glacier mass balance in the Cordillera Blanca, Peru: a review, AUC Geogr., 53 (2018) 106–118.

[4] C. Huggel, A. Kääb, W. Haeberli, P. Teysseire, F. Paul, Remote sensing based assessment of hazards from glacier lake outbursts: a case study in the Swiss Alps, Can. Geotech. J., 39 (2002) 316–330.

[5] K.R. Praveen, N.M. Varun, Changes of glacier lakes using multi-temporal remote sensing data: a case study from India, Geogr. Pannonica, 21 (2017) 132–141.

[6] I. Barisin, S. Leprince, B. Parsons, T. Wright, Surface displacements in the September 2005 Afar rifting event from satellite image matching: asymmetric uplift and faulting, Geophys. Res. Lett., 36 (2009) L07301, doi: 10.1029/2008GL036431.

[7] E.W. Burgess, R.R. Forster, C.F. Larsen, Flow velocities of Alaskan glaciers, Nat. Commun., 4 (2013) 2146, doi: 10.1038/ncomms3146.

[8] J. Huang, B. Yang, S.G. Lei, K.Z. Deng, Time-series SBAS pixel offset tracking method for monitoring three-dimensional deformation in a mining area, IEEE Access, 8 (2020) 118787–118798.

[9] H.Y. Jia, Y.J. Wang, D.Q. Ge, Y.K. Deng, R. Wang, Improved offset tracking for predisaster deformation monitoring of the 2018 Jinsha River landslide (Tibet, China), Remote Sens. Environ., 247 (2020) 111899, doi: 10.1016/j.rse.2020.111899.

[10] C.-H. Lu, Y.-S. Lin, R.Y. Chuang, Pixel offset fusion of SAR and optical images for 3-D coseismic surface deformation, IEEE Geosci. Remote Sens. Lett., 18 (2021) 1049–1053.

[11] M.F. Azam, P. Wagnon, E. Berthier, C. Vincent, K. Fujita, J.S. Kargel, Review of the status and mass changes of Himalayan-Karakoram glaciers, J. Glaciol., 64 (2018) 61–74.

[12] J. Li, Z.-W. Li, L.-X. Wu, B. Xu, J. Hu, Y.-S. Zhou, Z.-L. Miao, Deriving a time series of 3D glacier motion to investigate interactions of a large mountain glacial system with its glacial lake: use of synthetic aperture radar pixel offset-small baseline subset technique, J. Hydrol., 559 (2018) 596–608.

[13] H.N. Wang, Z.M. Zhou, J. Turnbull, Q. Song, F. Qi, Pol-SAR Classification based on generalized polar decomposition of Mueller matrix, IEEE Geosci. Remote Sens. Lett., 13 (2016) 565–569.

[14] B. Zhang, R. Zhang, G.X. Liu, Q. Liu, J.L. Cai, B. Yu, Y. Fu, Z.L. Li, Monitoring of interannual variabilities and outburst regularities analysis of Glacial Lakes at the End of Gongba glacier utilizing SAR images, Geomatics Inf. Sci. Wuhan Univ., 44 (2019) 1054–1064.

[15] R.L. Yang, B.W. Dai, L.L. Tan, X.Q. Liu, Z. Yang, H.Y. Li, Polarimetric Microwave Imaging: Polarimetric Microwave Imaging, Springer, Singapore, 2021.

[16] L. Mascolo, S.R. Cloude, J.M. Lopez-Sanchez, Model-based decomposition of dual-Pol SAR data: application to Sentinel-1, IEEE Trans. Geosci. Remote Sens., 60 (2021) 5220119, doi: 10.1109/TGRS.2021.3137588.

[17] Y.-p. Fang, The effects of natural capital protection on pastoralist's livelihood and management implication in the source region of the Yellow River, China, J. Mountain Sci., 10 (2013) 885–897.

[18] X.B. Wu, Q.L. Li, J.Q. He, Composition characteristics and its environmental implication of insoluble microparticles in snow cover on Yehelong glacier, Mt. Anyemaqen, source region of the Yellow River, J. Glaciol. Geocryology, 43 (2021) 1746–1754.

[19] G.F. De Grandi, M. Leysen, J.S. Lee, D. Schuler, Radar Reflectivity Estimation Using Multiple SAR Scenes of the Same Target: Technique and Applications, IGARSS'97. 1997 IEEE International Geoscience and Remote Sensing Symposium Proceedings. Remote Sensing - A Scientific Vision for Sustainable Development, IEEE, Singapore, 1997.

[20] S.R. Cloude, Polarisation: Applications in Remote Sensing, Oxford University, 2009.

[21] S.R. Cloude, E. Pottier, An entropy based classification scheme for land applications of polarimetric SAR, IEEE Trans. Geosci. Remote Sens., 35 (1997) 68–78.

[22] R.V. Engeset, J. Kohler, K. Melvold, B. Lundén, Change detection and monitoring of glacier mass balance and facies using ERS SAR winter images over Svalbard, Int. J. Remote Sens., 23 (2002) 2023–2050.

[23] J.J. van Zyl, Application of Cloude's Target Decomposition Theorem to Polarimetric Imaging Radar Data, Proceedings of SPIE - The International Society for Optical Engineering, 1993, pp. 184–191, doi: 10.1117/12.140615.

[24] V. Akbari, A.P. Doulgeris, T. Eltoft, Monitoring glacier changes using multi-temporal multi-polarization SAR images, IEEE Trans. Geosci. Remote Sens., 52 (2014) 3729–3741.

[25] S.L. Durden, J.J. van Zyl, H.A. Zebker, Modeling and observation of the radar polarization signature of forested areas, IEEE Trans. Geosci. Remote Sens., 27 (1989) 290–301.